

# Stochastic Search of the Quantum Conformational Space of Small Lithium and Bimetallic Lithium–Sodium Clusters

Jhon F. Pérez,<sup>†</sup> Elizabeth Florez,<sup>‡</sup> Cacier Z. Hadad,<sup>†</sup> Patricio Fuentealba,<sup>§</sup> and Albeiro Restrepo<sup>\*,†</sup>

*Grupo de Química-Física Teórica, Instituto de Química, Universidad de Antioquia, AA 1226 Medellín, Colombia, Grupo de Química de Recursos Energéticos y Medio Ambiente, Instituto de Química, Universidad de Antioquia, AA 1226 Medellín, Colombia, Departamento de Física, Facultad de Ciencias, Universidad de Chile, Casilla 653, Santiago 1, Chile*

Received: March 12, 2008; Revised Manuscript Received: April 12, 2008

In this paper we report the results obtained by an implementation and application of the simulated annealing optimization procedure to the exploration of the conformational space of small neutral and charged lithium clusters ( $\text{Li}_n^q$ ,  $n = 5, 6, 7$ ;  $q = 0, \pm 1$ ) and of the bimetallic lithium/sodium clusters ( $\text{Li}_5\text{Na}$ ) in their lowest spin states. Our methodology eliminates the structure guessing procedure in the process of generating cluster configurations. We evaluate the quantum energy, typically with the Hartree–Fock Hamiltonian, of randomly generated points in the conformational space and use a modified Metropolis test in the annealing algorithm to generate candidate structures for atomic clusters. The structures are further optimized by analytical methods (gradient following) at the Møller–Plesset second order perturbation theory level (MP2), in conjunction with basis sets including polarization functions with and without diffuse functions. High accuracy ab initio energies at the coupled clusters level, with single, double, and triple substitutions from the Hartree–Fock determinant (CCSD(T)), on the MP2 geometries were calculated and used to establish the relative stability of the isomers within each potential energy surface. Various cluster properties were computed and compared to existing values in order to validate our methods. Our results show excellent agreement with previous experimental and theoretical reports. Even at these small sizes, evidence for 10 new structures never reported before for the lithium clusters and four new structures for the bimetallic clusters is presented.

## 1. Introduction

Cluster science is an intensive subject of research in experimental and theoretical chemistry, physics, engineering, and material science, with implications in areas as diverse as catalysis,<sup>1–3</sup> molecular electronics,<sup>4–6</sup> nanotechnology,<sup>7</sup> hydrogen bonding,<sup>8–12</sup> and others. At a fundamental level, cluster properties and behavior represent a transition from atoms and molecules to bulk matter.

It is common to find potential energy surfaces (PES) that exhibit several local minima within a small range of energy corresponding to distinct geometrical motifs.  $\text{Li}_6$  clusters are a typical example: there are at least three structurally different isomers lying so close in energy that computational methods with modest treatment of electron correlation give conflicting results regarding relative energies. Sophisticated CCSD(T) calculations with large basis sets were needed to establish their relative stabilities as stated by Temelso and Sherrill.<sup>13</sup>

Since the structure of clusters determine many of their measurable properties, a good knowledge of the possible conformations and their relative energies is of primordial importance; however, structural issues are among the most difficult to tackle in the study of clusters. For small size clusters, systematic, intuition-guided construction of geometries until exhaustion of possibilities seems to be the methodology of

choice. An alternative plan, employed by Miyake and Aida in the study of small water clusters,<sup>14</sup> is to construct all the topologically distinct patterns for the system in question. In a different approach, Zope and co-workers<sup>15</sup> used known sodium cluster geometries as a starting point to study lithium clusters. The methods described above quickly become impracticable because the number of stationary points in a given potential energy surface (PES) increases dramatically as a function of size.<sup>16,17</sup>

In general, sampling of conformational spaces to determine equilibrium geometries is carried out by two different approaches: analytical (gradient following) and stochastic methods. The decision to choose one over the other depends on factors such as computational power, size of the system, and desired level of accuracy. A few characteristics of both methods are worth pointing out:<sup>16</sup> analytical methods produce very good quality stationary points with low frequency of evaluation of the gradient and the energy function. However, analytical methods can not jump over energy barriers, affording minima that are initial-guess-dependent; thus, a previous knowledge of the PES is required in order not to get trapped in undesired local minima. These features make analytical methods suitable for the treatment of small systems with high levels of theory. A recent implementation of the Car–Parrinello molecular dynamics (CPMD) by Iannuzzi and co-workers<sup>18</sup> allows the possibility of jumping over energy barriers; however, the authors pointed out efficiency issues that are specific-problem-dependent and concerns about the significant amount of information required as input for a successful exploration of a given PES. On the other hand, stochastic methods randomly search the

\* Corresponding author. E-mail: albeiro@matematicas.udea.edu.co.

<sup>†</sup> Grupo de Química-Física Teórica, Universidad de Antioquia.

<sup>‡</sup> Grupo de Química de Recursos Energéticos y Medio Ambiente, Universidad de Antioquia.

<sup>§</sup> Departamento de Física, Universidad de Chile.

conformational space to produce structures that often need refinement to locate stationary points. Stochastic methods are initial-guess-independent, can jump over energy barriers, and so have the ability to sample several wells in the same run. The random nature of the search implicitly carries the need for repetitive evaluation of the energy function. Thus, stochastic methods have traditionally been used to study large systems with low levels of theory. The advances in technology that have produced faster and more powerful computers have allowed the recent implementation of stochastic methods with energy evaluated via quantum Hamiltonians,<sup>19–23</sup> which amounts to a better treatment of electron interaction. This paper is an example of such an approach with direct application to small lithium and bimetallic lithium–sodium clusters.

Lithium clusters have been extensively studied from a theoretical standpoint partially because lithium atoms, which contain three electrons, are among the smallest atoms that can form metallic clusters (hydrogen atom clusters exhibit metallic character under extreme pressures). The large variety of methods used to study lithium clusters includes, among others, several flavors of DFT,<sup>21,24–28</sup> configuration interaction,<sup>27,29–32</sup> MP2,<sup>27,33</sup> coupled clusters,<sup>13,21,27,34</sup> CASSCF,<sup>27</sup> generalized valence bond theory,<sup>35–37</sup> ab initio molecular dynamics,<sup>38</sup> ab initio path integral methods,<sup>27,39,40</sup> variational quantum Monte Carlo methods,<sup>41</sup> and Gradient embedded genetic algorithms.<sup>21</sup> Several works have shown that electron correlation energy is an essential contribution to cluster stability.<sup>29,30,42–44</sup> Boustani and Koutecký determined that geometries for anionic lithium clusters differ appreciably from those of neutral and cationic clusters.<sup>45</sup> From molecular orbital analysis of the chemical bonding in lithium clusters, Alexandrova and Boldyrev established that multiple  $\pi$  and  $\sigma$  aromaticity play significant roles as major stabilizing effects.<sup>21</sup> Visser and co-workers<sup>46</sup> reported that high-spin lithium clusters, despite having no bonding electron pairs, exhibit rich conformational spaces, with clusters being held together via multiplet interactions. Regarding structural issues, for homo-nuclear metallic clusters  $M_n$ ,  $n = 6$  seems to be the transition point from planar ( $n < 6$ ) to 3D ( $n > 6$ ) structural preference.<sup>13,47,48</sup>

In this work, we develop a strategy for generating local minima candidate cluster structures; our procedure bypasses the guessing process when locating stationary points within a given PES. We use a locally implemented version of the simulated annealing algorithm<sup>49–51</sup> that evaluates the energy by quantum methods at each randomly generated nuclear configuration (see Computational Methods section for details). Each candidate is then refined by analytical methods to locate the closest stationary point upon which high-accuracy energies are calculated. Particular application to small charged and neutral lithium clusters in their lowest spin states ( $Li_n^q$ ,  $n = 5, 6, 7$ ;  $q = 0, \pm 1$ ), for which extensive data exist in the literature, is used as a means to validate our methods. The bimetallic  $Li_5Na$  clusters are also studied.

## 2. Computational Methods

We implemented an adapted version of the simulated annealing (SA) optimization algorithm<sup>49–51</sup> into the ASCEC (Spanish acronym for annealing simulado con energía cuántica) program.<sup>52</sup> At present, the program is capable of simulating atomic and molecular clusters.

**2.1. The Annealing Procedure: A Brief Description of the Workings of ASCEC.** The system is allowed to evolve inside a cubic box of user supplied length  $L$ , in agreement with the original algorithm proposed by Metropolis et al.<sup>49</sup> The ASCEC program calls on the Gaussian 03 suite of programs<sup>53</sup> to calculate the

quantum energy of every generated structure which is then the subject of an acceptance test. If the structural change lowers the energy ( $\Delta E < 0$ ), then the move is accepted; when  $\Delta E > 0$ , the new structure is accepted if  $\Phi(\Delta E) < P(\Delta E)$ , where  $P(\Delta E) = \exp(-\Delta E/k_B T)$  is the temperature-dependent Boltzmann's probability distribution function and  $\Phi(\Delta E) = |\Delta E/E_j|$ ,  $j$  being the structure under evaluation. We found the latter acceptance criterion to be more adequate in this line of problems than the usual procedure of comparing  $P(\Delta E)$  to a randomly generated number in the  $[0,1]$  range, where good structures can be randomly rejected. If neither test is satisfied, the move is not accepted and the structure that originated the change is randomly modified again. To avoid a large number of meaningless energy evaluations, a maximum number of structures can be generated at each temperature without satisfying either of the two acceptance criteria; that number (MaxCyc) is reduced every time it is reached. Atom positions of a particular structure are simultaneously moved at random up to a maximum displacement allowed. Only accepted structures are changed, effectively constructing a Markov chain of points in the conformational space.

A typical run of ASCEC requires the following user supplied information: (a) a quenching route [initial and final temperatures and a route connecting them; at present, a choice between linear (decreasing  $T$  by a constant amount) and geometric (decreasing  $T$  by a constant percentage) routes is available], (b) the initial geometry in Cartesian coordinates, (c) a length for a cube in which the system evolves, (d) the maximum initial number of structures to be evaluated before going to the next temperature (MaxCyc), (e) the maximum allowed atom displacements, and (f) a combination of Hamiltonian/basis set for energy calculations. The entire process of input generation for the Gaussian 03 calculations and the processing of its outputs is completely transparent to the user, so only ASCEC-related files are to be manipulated. In this research, we found the HF/lanl2dz level of theory to be a good compromise between speed and accuracy, so unless otherwise indicated, it is the methodology of choice for energy calculations during ASCEC runs. Lanl2dz comprises an all-electron calculation for lithium atoms that includes double- $\zeta$  plus polarization.<sup>54–57</sup>

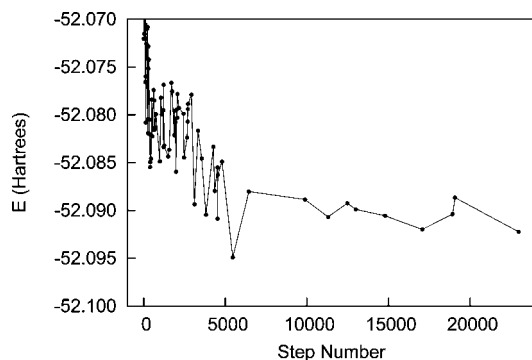
**2.2. Locating and Treating Stationary Points.** A successful ASCEC run generates a number of candidate structures; only those typically lying up to about 0.02 hartree above the lowest energy were selected to be optimized by analytical methods. For computational efficiency, the BLYP functional in conjunction with the lanl2dz basis set was used to optimize the structures generated by the ASCEC program. Because many initial structures converged to the same equilibrium geometry, just a few stationary points were found by this procedure. To have a better treatment of electron correlation, the stationary points located with BLYP/lanl2dz were further refined at the more sophisticated MP2/6-311g(d) and MP2/6-311+g(d) levels. Analytical harmonic second-derivative calculations at the same MP2 levels were used to characterize stationary points as true minima (no negative eigenvalues of the Hessian matrix) or saddle points. As previously suggested,<sup>13,21,27,34</sup> high-accuracy CCSD(T) energy calculations were carried out in order to establish the relative stability of the isomers. Exclusion of diffuse functions is of no consequence in the study of small lithium anionic clusters, as pointed out by Temelso and Sherrill.<sup>13</sup>

Following standard procedures (see, for example, ref 29) binding energies per atom are calculated as  $BE/atom = (nE_1 - E_n)/n$  for neutral clusters and  $BE/atom = [(n - 1)E_1 + E_1^q - E_n]/n$  for charged clusters. Adiabatic ionization potentials are

TABLE 1: ASCEC Entry Parameters and Results

parameter	Li <sub>5</sub> <sup>+</sup>	Li <sub>5</sub>	Li <sub>5</sub> <sup>-</sup>	Li <sub>6</sub> <sup>+</sup>	Li <sub>6</sub>	Li <sub>6</sub> <sup>-</sup>	Li <sub>7</sub> <sup>+</sup>	Li <sub>7</sub>	Li <sub>7</sub> <sup>-</sup>
MaxCyc <sup>a</sup>	2000	2000	2000	2000	5000	2000	5000	5000	5000
generated structures	64	49	80	156	111	61	37	33	89
with $\Delta E < 0$	7	14	10	11	10	10	12	8	14
with $\Phi(\Delta E) < P(\Delta E)$	57	35	70	145	101	51	25	25	75
candidate structures <sup>b</sup>	54	32	63	67	84	22	11	25	66
located minima	2	2	3	4	3	7	2	2	3

<sup>a</sup> See Annealing Procedure section. <sup>b</sup> Within 0.02 hartree of lowest energy.

Figure 1. Simulated annealing for Li<sub>7</sub><sup>-</sup> clusters.

calculated as the difference in energy between the optimized geometries for the lowest energy cationic and neutral clusters. Vertical ionization potentials are calculated as the difference between the energy of the neutral cluster and the energy of the cation in the optimized neutral cluster geometry. Isomer populations,  $x_i$ , within a given cluster were estimated by<sup>58</sup>

$$x_i = \frac{g_i e^{-E_i/k_B T}}{\sum_i g_i e^{-E_i/k_B T}} \quad (1)$$

where  $g_i$  is the symmetry number for isomer  $i$  (its degeneracy) and  $E_i$  the corresponding CCSD(T)//MP2 energy. All geometry optimizations, frequency, and energy calculations were carried out using the Gaussian 03<sup>53</sup> suite of programs.

### 3. Results and Discussion

**3.1. ASCEC Results.** Initial geometries for all ASCEC runs were constructed with atoms located at the same position (this procedure is dubbed the big bang approach), allowing them to evolve under the annealing conditions within a cube of 7 Å of length. The HF/lanl2dz formalism was used to calculate energies of randomly generated cluster configurations. All runs used a geometric quenching route with initial temperature of 500 K, a constant decrease of 5%, and 50 total temperatures. Table 1 summarizes the details about ASCEC runs for lithium clusters. It can be seen that most of the candidate structures were generated after satisfying our modified Metropolis test [ $\Phi(\Delta E) < P(\Delta E)$ ], while few structures were accepted after a random move resulted in a lower energy configuration.

Figure 1 shows an energy profile for the ASCEC run of the Li<sub>7</sub><sup>-</sup> clusters. The ability of the algorithm to jump over energy barriers is clearly seen in the nonmonotonical decrease in energy as the simulation proceeds. Most of the accepted structures happen in early to intermediate stages of the annealing. As the temperature lowers, the frequency of structure acceptance decreases because satisfying either of the two criteria is increasingly harder. In Figure 2 we plotted the energy of the structures produced by the annealing as a function of their temperature for the same Li<sub>7</sub><sup>-</sup> clusters. The simulation runs down

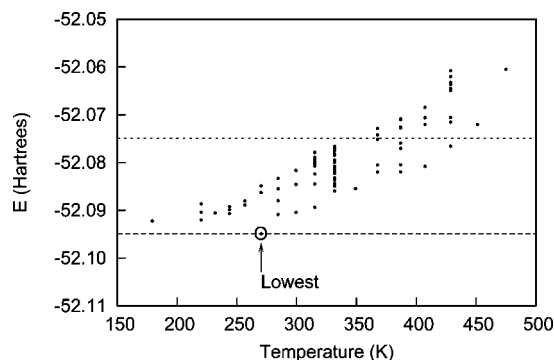


Figure 2. Candidate structures generated by the annealing. Only those within 0.02 hartree (between dashed lines) of the lowest energy are considered for optimization.

TABLE 2: Structural Motifs for Lithium Clusters<sup>a</sup>

cluster	structures and references
Li <sub>5</sub> <sup>+</sup>	$D_{2d}$ , <sup>21</sup> $D_{3h}$ , <sup>21,29</sup> $D_{2h}$ , <sup>29</sup> $c$
Li <sub>5</sub>	$C_{2v}$ , <sup>21,29</sup> $C_{2v}$ , <sup>b</sup> $C_{2v}$ , <sup>21,29</sup> $c,d$ $D_{3h}$ , <sup>c</sup>
Li <sub>5</sub> <sup>-</sup>	$C_{2v}$ , <sup>21,45</sup> $C_{2v}$ , <sup>d</sup> $C_{4v}$ , <sup>21</sup>
Li <sub>6</sub> <sup>+</sup>	$D_{2h}$ , <sup>13,21,29</sup> $D_{2d}$ , <sup>a,b</sup> $D_{2d}$ , <sup>b</sup> $D_{3h}$ , <sup>b</sup>
Li <sub>6</sub>	$C_{5v}$ , <sup>13,21,29,38</sup> $D_{3h}$ , <sup>13,21,29,33,38</sup> $D_{4h}$ , <sup>13,21,33</sup>
Li <sub>6</sub> <sup>-</sup>	$D_{3h}$ , <sup>45</sup> $D_{4h}$ , <sup>13,21</sup> $C_{s}$ , <sup>a</sup> $C_{s}$ , <sup>b</sup> $D_{2h}$ , <sup>b</sup> $D_{3h}$ , <sup>b</sup> $D_{\infty h}$ , <sup>b</sup>
Li <sub>7</sub> <sup>+</sup>	$C_{3v}$ , <sup>29</sup> $D_{5h}$ , <sup>21,29</sup>
Li <sub>7</sub>	$C_{3v}$ , <sup>a</sup> $D_{5h}$ , <sup>21,29</sup>
Li <sub>7</sub> <sup>-</sup>	$C_{3v}$ , <sup>a,b</sup> $C_{3v}$ , <sup>b</sup> $D_{5h}$ , <sup>21,45</sup>

<sup>a</sup> See Figures 3, 4, and 5 for geometries. <sup>b</sup> Never before reported. <sup>c</sup> Not found from the SA. <sup>d</sup> Located starting from the  $C_{2v,c}$  geometry in ref 29.

to 40.5 K, with the last accepted configuration happening at 179.2 K. Structures lying above 0.02 hartree (above the upper dashed line, Figure 2) of the lowest energy structure are discarded for further optimization. It can be seen from both Figures 1 and 2 that the lowest energy structure was not found at the lowest simulation temperature. All the observations in this paragraph are consistent with what is expected from a robust and efficient implementation of the annealing algorithm.

**3.2. Lithium Clusters.** The MP2 equilibrium geometries were generated following the procedure described in the Methodology section. It is important to point out that all geometry optimizations were carried out without imposing symmetry constraints, as the candidate structures coming from ASCEC are randomly generated and belong to the  $C_1$  point group; however the stationary points reached from them have higher symmetries.<sup>59</sup> All lithium cluster geometries found in this and other works are listed in Table 2 along with the most representative references in each case.

**3.2.1. Geometries.** The several structural motifs for Li<sub>5</sub><sup>q</sup>, Li<sub>6</sub><sup>q</sup>, and Li<sub>7</sub><sup>q</sup> clusters are depicted in Figures 3, 4, and 5, respectively. Their corresponding geometrical parameters are listed in Table 3. From Table 2, a total of 10 structures never before reported have been predicted with our methodology, while two previously reported conformations, found with different levels of theory,

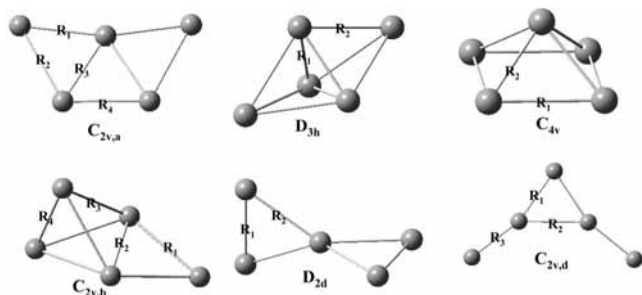


Figure 3. Geometrical motifs for neutral and charged  $\text{Li}_5$  clusters.

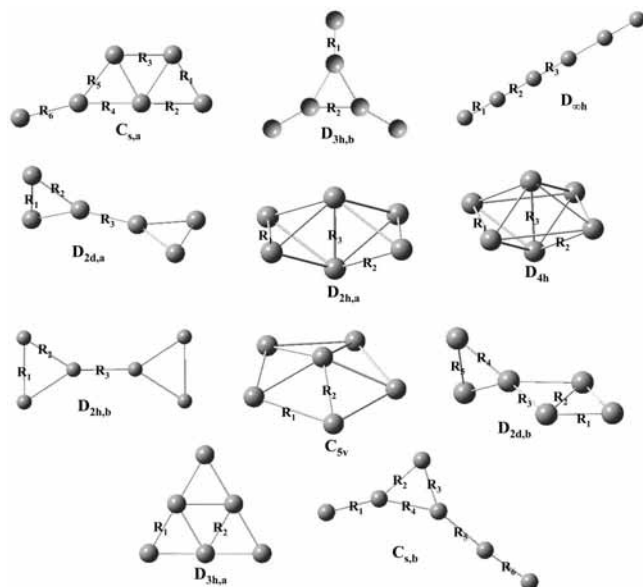


Figure 4. Geometrical motifs for neutral and charged  $\text{Li}_6$  clusters.

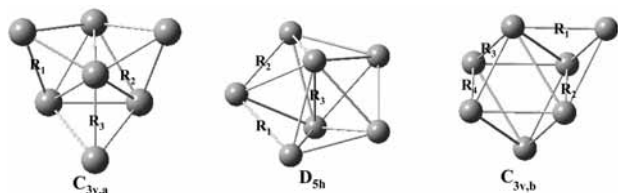


Figure 5. Geometrical motifs for neutral and charged  $\text{Li}_7$  clusters.

were not located. The  $D_{2h}$  structure for the  $\text{Li}_5^+$  cluster has been reported only once in the literature;<sup>29</sup> it was found at the HF level using a minimal basis augmented with one p polarization function. Efforts to locate a corresponding conformation within the MP2 PESs afforded no stable minima (one structure was found with the same symmetry having one imaginary frequency). We located the missing  $C_{2v,c}$  cluster for  $\text{Li}_5$  reported in refs 21, 29 starting with a geometry that resembles the one found in an earlier paper by Boustani et al.<sup>29</sup>

For  $\text{Li}_5^q$  clusters, a total of seven stationary points are located, two for  $\text{Li}_5^+$ , two for  $\text{Li}_5$ , and three for  $\text{Li}_5^-$ . Three are planar and four are nonplanar. One new nonplanar structure ( $C_{2v,b}$  in Figure 3) is found for the neutral cluster. For  $\text{Li}_6^q$  clusters, 14 structures were found, four for  $\text{Li}_6^+$ , three for  $\text{Li}_6$ , and seven for  $\text{Li}_6^-$ . Eight are planar and six are nonplanar. Three new structures, one planar ( $D_{3h,b}$  in Figure 4) and two nonplanar ( $D_{2d,a}$  and  $D_{2d,b}$  in Figure 4), are found for the cationic cluster, while five new planar structures ( $C_{s,a}$ ,  $C_{s,b}$ ,  $D_{2h,b}$ ,  $D_{3h,b}$ , and  $D_{\infty h}$  in Figure 4) are found for the anionic cluster. No new structures were found for the neutral cluster. For  $\text{Li}_7^q$  clusters, There is no planarity in the seven structures predicted for the

TABLE 3: Atom Distances ( $\text{\AA}$ ) for  $\text{Li}_n^q$  Clusters<sup>a</sup>

cluster	$R_1$	$R_2$	$R_3$	$R_4$	$R_5$	$R_6$
$\text{Li}_5^q$						
$\text{Li}_5^+$ , $D_{3h}$	2.76	3.21				
$\text{Li}_5^+$ , $D_{2d}$	2.88	3.12				
$\text{Li}_5$ , $C_{2v,a}$	3.00	3.11	2.91	3.08		
$\text{Li}_5$ , $C_{2v,b}$	3.04	2.96	3.10	2.72		
$\text{Li}_5^-$ , $C_{2v,a}$	3.00	3.31	2.97	3.02		
$\text{Li}_5^-$ , $C_{4v}$	3.26	2.85				
$\text{Li}_5^-$ , $C_{2v,d}$	3.07	3.46	2.96			
$\text{Li}_6^q$						
$\text{Li}_6^+$ , $D_{2h,a}$	3.19	3.01	2.60			
$\text{Li}_6^+$ , $D_{2d,b}$	3.03	2.70	3.42	3.05	2.95	
$\text{Li}_6^+$ , $D_{2d,a}$	2.93	3.06	3.19			
$\text{Li}_6^+$ , $D_{3h,b}$	3.13	3.23				
$\text{Li}_6$ , $D_{4h}$	3.61	2.87	2.63			
$\text{Li}_6$ , $C_{5v}$	3.18	2.88				
$\text{Li}_6$ , $D_{3h,a}$	3.02	3.06				
$\text{Li}_6^-$ , $D_{4h}$	3.38	2.90	3.27			
$\text{Li}_6^-$ , $C_{s,a}$	3.02	3.25	3.06	3.30	3.17	3.16
$\text{Li}_6^-$ , $D_{3h,a}$	2.97	3.00				
$\text{Li}_6^-$ , $D_{s,b}$	2.95	3.13	2.92	3.31	3.29	2.97
$\text{Li}_6^-$ , $D_{\infty h}$	2.93	3.26	3.15			
$\text{Li}_6^-$ , $D_{3h,b}$	2.90	3.33				
$\text{Li}_6^-$ , $D_{2h,b}$	3.25	2.97	3.11			
$\text{Li}_7^q$						
$\text{Li}_7^+$ , $D_{5h}$	3.26	3.04	2.52			
$\text{Li}_7^+$ , $C_{3v,a}$	3.09	3.31	3.27	2.78		
$\text{Li}_7$ , $D_{5h}$	3.09	3.00	2.85			
$\text{Li}_7$ , $C_{3v,a}$	3.17	3.07	2.97	2.75		
$\text{Li}_7^-$ , $D_{5h}$	2.93	3.06	3.55			
$\text{Li}_7^-$ , $C_{3v,b}$	2.94	3.15	2.95	3.13		
$\text{Li}_7^-$ , $C_{3v,a}$	3.09	2.96	2.80	3.05		

<sup>a</sup> For variable definition, see Figures 3, 4, and 5.

clusters, two for  $\text{Li}_7^+$ , two for  $\text{Li}_7$ , and three for  $\text{Li}_7^-$ . One new structure ( $C_{3v,a}$  in Figure 5) was found for  $\text{Li}_7^-$ . These results seem to agree with the nonplanarity structural preference for homonuclear metallic clusters with more than six atoms.<sup>13,47,48</sup>

Our method predicts a number of unreported structures. However, there are no significant differences between our geometries and those reported previously by others. For instance, in the most recent lithium clusters report by Alexandrova and Boldyrev,<sup>21</sup> they found for the  $\text{Li}_5^+$ ,  $D_{3h}$  structure atom distances of 2.69, 2.77  $\text{\AA}$  for  $R_1$  and 3.15, 3.16  $\text{\AA}$  for  $R_2$  at the B3LYP/6-311+g(d), CCSD(T)/6-311+g(d) levels, respectively, while we found (Table 3, Figure 3) 2.76 and 3.21  $\text{\AA}$  for the same variables using the MP2/6-311g(d) formalism. The anions show a wider variety of structural possibilities than the neutral and cationic clusters with the same number of atoms, an observation already pointed out by Boustani and Koutecký.<sup>45</sup> For clusters with an equal number of atoms that exhibit the same structural motifs for different charge numbers, some geometrical changes are observed as a consequence of the cluster having to accommodate a varying number of electrons. The most dramatic case comes from the comparison between the  $D_{5h}$  geometries of the  $\text{Li}_7^+$ ,  $\text{Li}_7$ , and  $\text{Li}_7^-$  clusters (Table 3): the distance between the two out of plane atoms increases from 2.52 to 2.85 to 3.55  $\text{\AA}$ , while the other distances change in a somewhat smoother fashion. Similar behavior is observed when comparing the  $D_{4h}$  neutral and anionic  $\text{Li}_6$  clusters (Table 3) and in the  $C_{3v,a}$  geometries of the cationic, neutral, and anionic  $\text{Li}_7$  clusters (Table 3).

Other methods for searching the potential energy surfaces of the clusters under study yielded somewhat similar results. Specifically, ab initio molecular dynamics performed on  $\text{Li}_6$

TABLE 4: Energies (kcal/mol) for Pure Li Clusters<sup>a</sup>

cluster	MP2		CCSD(T)//MP2		
	$\Delta E$	BE/atom	$\Delta E$	BE/atom	pop <sup>b</sup> ( $\approx\%$ )
Li <sub>5</sub> <sup>q</sup>					
Li <sub>5</sub> <sup>+</sup> , <i>D</i> <sub>3h</sub>	0.00	19.30	0.00	22.78	99.77
Li <sub>5</sub> <sup>+</sup> , <i>D</i> <sub>2d</sub>	2.07	18.89	3.64	22.05	0.23
Li <sub>5</sub> , <i>C</i> <sub>2v,c</sub>	0.78	11.25	0.00	16.53	76.25
Li <sub>5</sub> , <i>C</i> <sub>2v,a</sub>	0.00	11.41	0.70	16.39	23.74
Li <sub>5</sub> , <i>C</i> <sub>2v,b</sub>	3.03	10.80	5.62	15.41	0.01
Li <sub>5</sub> <sup>-</sup> , <i>C</i> <sub>2v,a</sub>	1.33	14.88	0.00	18.03	67.85
Li <sub>5</sub> <sup>-</sup> , <i>C</i> <sub>4v</sub>	0.00	15.15	0.45	17.94	32.05
Li <sub>5</sub> <sup>-</sup> , <i>C</i> <sub>2v,d</sub>	6.34	13.88	3.91	17.25	0.10
Li <sub>6</sub> <sup>q</sup>					
Li <sub>6</sub> <sup>+</sup> , <i>D</i> <sub>2h,a</sub>	0.00	19.57	0.00	23.10	100.00
Li <sub>6</sub> <sup>+</sup> , <i>D</i> <sub>2d,b</sub>	13.40	17.33	12.92	20.95	0.00
Li <sub>6</sub> <sup>+</sup> , <i>D</i> <sub>2d,a</sub>	15.04	17.06	14.11	20.75	0.00
Li <sub>6</sub> <sup>+</sup> , <i>D</i> <sub>3h,b</sub>	29.25	14.69	36.03	17.09	0.00
Li <sub>6</sub> , <i>D</i> <sub>4h</sub>	0.00	15.14	0.00	18.50	73.86
Li <sub>6</sub> , <i>C</i> <sub>5v</sub>	4.59	14.37	0.68	18.38	23.94
Li <sub>6</sub> , <i>D</i> <sub>3h,a</sub>	7.16	13.94	2.10	18.15	2.21
Li <sub>6</sub> <sup>-</sup> , <i>D</i> <sub>4h</sub>	0.00	17.32	0.00	20.31	100.00
Li <sub>6</sub> <sup>-</sup> , <i>C</i> <sub>s,a</sub>	26.91	12.84	15.86	17.66	0.00
Li <sub>6</sub> <sup>-</sup> , <i>D</i> <sub>3h,a</sub>	21.21	13.78	17.31	17.42	0.00
Li <sub>6</sub> <sup>-</sup> , <i>C</i> <sub>s,b</sub>	26.19	12.96	21.00	16.81	0.00
Li <sub>6</sub> <sup>-</sup> , <i>D</i> <sub>∞h</sub>	24.91	13.17	22.82	16.50	0.00
Li <sub>6</sub> <sup>-</sup> , <i>D</i> <sub>3h,b</sub>	26.74	12.86	23.45	16.40	0.00
Li <sub>6</sub> <sup>-</sup> , <i>D</i> <sub>2h,b</sub>	41.28	10.44	47.05	12.47	0.00
Li <sub>7</sub> <sup>q</sup>					
Li <sub>7</sub> <sup>+</sup> , <i>D</i> <sub>5h</sub>	0.00	21.64	0.00	25.10	99.99
Li <sub>7</sub> <sup>+</sup> , <i>C</i> <sub>3v,a</sub>	6.40	20.73	5.29	24.34	0.01
Li <sub>7</sub> , <i>D</i> <sub>5h</sub>	0.00	15.74	0.00	20.52	100.00
Li <sub>7</sub> , <i>C</i> <sub>3v,a</sub>	6.02	14.88	7.79	19.96	0.00
Li <sub>7</sub> <sup>-</sup> , <i>D</i> <sub>5h</sub>	0.00	19.38	0.00	21.94	77.64
Li <sub>7</sub> <sup>-</sup> , <i>C</i> <sub>3v,b</sub>	1.97	19.10	0.78	21.82	21.06
Li <sub>7</sub> <sup>-</sup> , <i>C</i> <sub>3v,a</sub>	3.66	18.86	2.45	21.59	1.31

<sup>a</sup> All calculations with the 6-311g(d) basis set. Isomers are placed in descending order according to their CCSD(T)//MP2 stabilities. Experimental binding energies per atom are 24.21, 23.29, and 25.60 for Li<sub>5</sub>, Li<sub>6</sub>, and Li<sub>7</sub> clusters, respectively.<sup>60</sup> <sup>b</sup> Populations are estimated by equation 1.

TABLE 5: MP2/6-311g(d) Calculated Properties for Pure Li Clusters<sup>a</sup>

cluster	ionization potential			polarizability	
	adiabatic	vertical <sup>b</sup>	experimental <sup>c</sup>	calculated	experimental <sup>c</sup>
Li <sub>5</sub> , <i>C</i> <sub>2v,c</sub>	3.81	3.91	4.02 ± 0.05 <sup>61</sup>	345.55	427.5 <sup>62</sup>
Li <sub>5</sub> , <i>C</i> <sub>2v,a</sub>	3.61	4.07		459.80	
Li <sub>5</sub> , <i>C</i> <sub>2v,b</sub>	3.60	3.87		463.21	
Li <sub>6</sub> , <i>D</i> <sub>4h</sub>	4.18	4.47	4.20 ± 0.05 <sup>61</sup>	467.60	359.2 <sup>62</sup>
Li <sub>6</sub> , <i>C</i> <sub>5v</sub>	3.96	4.62		519.70	
Li <sub>6</sub> , <i>D</i> <sub>3h,a</sub>	3.84	4.82		526.80	
Li <sub>7</sub> , <i>D</i> <sub>5h</sub>	3.86	3.98	3.94 ± 0.05 <sup>61</sup>	523.40	539.0 <sup>62</sup>
Li <sub>7</sub> , <i>C</i> <sub>3v,a</sub>	3.29	3.76		360.60	

<sup>a</sup> All energies in eV. Polarizabilities in au. <sup>b</sup> Vertical IPs calculated with the 6-311+g(d) basis set are 4.45 eV for Li<sub>5</sub>, *C*<sub>2v,c</sub>; 4.61 eV for Li<sub>6</sub>, *D*<sub>4h</sub>; and 4.01 eV for Li<sub>7</sub>, *D*<sub>5h</sub>. <sup>c</sup> Experimental values are not for the particular isomer.

clusters resulted in the same geometries reported here.<sup>38</sup> Gradient embedded genetic algorithms (GEGA) applied to the same Li<sub>*n*</sub><sup>q</sup> of this study yielded fewer structures than our simulated annealing procedure.<sup>21</sup> To our knowledge, there are no other reports on systematic searches of the PES for the title systems.

**3.2.2. Energies and Other Properties.** Calculated relative and binding energies for all lithium clusters are listed in Table 4; other predicted properties are included in Table 5. Li<sub>5</sub> and Li<sub>5</sub><sup>-</sup> clusters are the only instances in which MP2 and CCSD(T)//MP2 do not predict the same global minimum. There is a

remarkable agreement between the two methods in the prediction of the most stable isomer in every other case. From our estimated populations, it can be seen that Li<sub>5</sub>, Li<sub>5</sub><sup>-</sup>, Li<sub>6</sub>, and Li<sub>7</sub><sup>-</sup> exhibit nondominant cluster configurations; in all the other cases, one isomer is predicted to be in abundances above 99%. For such cases, the global minima predicted by us are in agreement with previous reports,<sup>13,21</sup> except for the case of Li<sub>5</sub><sup>-</sup>, where Alexandrova and Boldyrev<sup>21</sup> predict the *C*<sub>4v</sub> structure to be more stable than the *C*<sub>2v,a</sub> by 0.3 kcal/mol, while our results give 0.45 kcal/mol in favor of the *C*<sub>2v,a</sub> isomer at the CCSD(T)/6-311g(d)//MP2/6-311g(d) level. In this case, the differences in energies are small enough to render the results inconclusive.

Some differences between the binding energies reported here and those found in the literature are observed. For the Li<sub>6</sub><sup>+</sup> cluster, the experimental binding energy per atom is 24.91 kcal/mol;<sup>60</sup> our CCSD(T)/6-311g(d)//MP2/6-311g(d) results predict 23.10 kcal/mol for the *D*<sub>2h,a</sub> isomer (the dominant configuration, Table 4), while Temelso and Sherrill's value at the CCSD(T)/cc-pCVDZ+diff level is 23.76 kcal/mol for a structure with *C*<sub>2v</sub> symmetry.<sup>13</sup> The very sophisticated study by Temelso and Sherrill predicts binding energies per atom in the *D*<sub>4h</sub> symmetry isomer of the Li<sub>6</sub><sup>-</sup> clusters to be 20.69 kcal/mol, while our value is 20.31 kcal/mol. Our results consistently underestimate the BE/atom for neutral clusters (see Table 4). For Li<sub>*n*</sub><sup>q</sup> (*n* = 5, 6, 7; *q* = 0, ±1), it is seen that cationic clusters have stronger binding energies than their anionic and neutral counterparts.

In Table 5, the calculated vertical and adiabatic ionization potentials and the dipole polarizabilities are displayed. It has been reported that electron correlation does not play a major role in the evaluation of polarizability in lithium clusters as opposed to sodium and other types of clusters.<sup>63</sup> Calculated values are compared with the experimental values. One can see that there is a noticeable difference between the vertical and the adiabatic ionization potentials as a consequence of the important geometrical distortion after ionization. The vertical ionization potentials, with the exception of that of Li<sub>6</sub>, are in fair agreement with the experimental values. Inclusion of a diffuse function does not improve the quality of the calculated vertical IPs. The dipole polarizabilities differ markedly of the experimental values. This deviation has already been discussed several times without a clear explanation until recently.<sup>64</sup>

**3.3. Li<sub>5</sub>Na Clusters.** As a more challenging case, we applied the methodology described above to the study of bimetallic Li<sub>5</sub>Na clusters in the lowest singlet spin states. In this problem, the symmetry of the homonuclear clusters is broken by the addition of the "impurity" (the sodium atom), making structure prediction a more difficult task. We also investigate the effect of adding diffuse functions, effectively using the 6-311g(d) and 6-311+g(d) basis sets.

**3.3.1. Geometries.** We obtained the three geometrical motifs depicted in Figure 6: two distorted octahedral geometries with the sodium atom occupying equatorial (*C*<sub>2v,a</sub>) or axial (*C*<sub>4v</sub>) positions, two pentagonal-based pyramids with the sodium atom sitting at the top (*C*<sub>5v</sub>) or on the plane (*C*<sub>s</sub>), and two planar structures with the sodium atom lying on the corner (*C*<sub>2v,b</sub>) or on the side (*C*<sub>2v,c</sub>). In a previous work, Desphande and co-workers<sup>65</sup> reported the *C*<sub>4v</sub> and *C*<sub>5v</sub> structures in Figure 6, obtained by means of ab initio molecular dynamics within the framework of DFT using the simulated annealing strategy; in the same paper, the existence of a planar pentagon with lithium atoms in the corners surrounding an in-plane central sodium atom is also mentioned, such structure is predicted not to be a true minimum in the MP2 PESs, because of the presence of one imaginary vibrational frequency. There are no differences

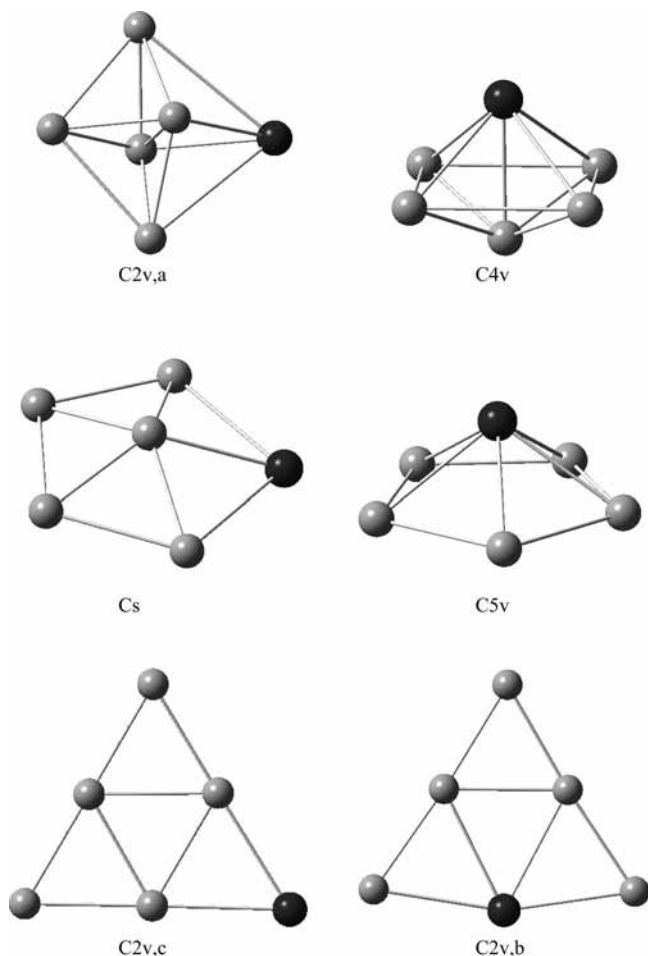


**Figure 6.** Geometrical motifs for  $\text{Li}_5\text{Na}$  clusters.

**TABLE 6: Energies (kcal/mol) for  $\text{Li}_5\text{Na}$  Clusters<sup>a</sup>**

cluster	MP2		CCSD(T)//MP2		
	$\Delta E$	BE/atom	$\Delta E$	BE/atom	pop <sup>b</sup> ( $\approx\%$ )
6-311g(d)					
$C_{2v,a}$	0.00	14.89	0.00	18.08	99.76
$C_s$	4.52	14.14	3.66	17.47	0.21
$C_{2v,b}$	6.71	13.78	4.77	17.29	0.03
$C_{2v,c}$	10.16	13.20	7.67	16.80	0.00
$C_{4v}$	8.89	13.41	8.33	16.69	0.00
$C_{5v}$	13.51	12.64	11.73	16.13	0.00
6-311g+(d)					
$C_{2v,a}$	0.00	14.93	0.00	18.12	99.79
$C_s$	4.59	14.17	3.73	17.50	0.18
$C_{2v,b}$	6.77	13.80	4.84	17.31	0.03
$C_{2v,c}$	10.22	13.23	7.74	16.83	0.00
$C_{4v}$	8.90	13.45	8.33	16.73	0.00
$C_{5v}$	13.56	12.67	11.78	16.15	0.00

<sup>a</sup> Isomers are placed in descending order according to their CCSD(T)//MP2 stabilities. <sup>b</sup> Populations estimated by eq 1. Vertical IP for the  $C_{2v,a}$  structure is 4.48 eV at the MP2/6-311g(d) level.

in the number nor in the conformations of the stationary points located using the 6-311g(d) and 6-311+g(d) basis sets. The geometrical distortion due to the presence of the sodium atom is more apparent in the Li–Na distances, which range from 3.14 to 3.46 Å in the bimetallic clusters, as opposed to distances no larger than 3.18 Å for the homonuclear clusters.

**3.3.2. Energies and Other Properties.** Table 6 summarizes energy-related results for the  $\text{Li}_5\text{Na}$  clusters. Our calculations favor nonplanar configurations, predicting the  $C_{2v,a}$  structure

to have the lowest energy, present in abundances above 99%, the CCSD(T)//MP2 stability order being  $C_{2v,a} > C_s > C_{2v,b} > C_{2v,c} > C_{4v} > C_{5v}$ . This result is in sharp contrast with the DFT findings of Desphande et al.,<sup>65</sup> which predict the  $C_{4v}$  and  $C_{5v}$  to be the most stable structures. It can be noticed by comparing Tables 4 and 6 and Figures 4 and 6 that the most stable  $\text{Li}_5\text{Na}$  structures are lower symmetry versions of the most stable  $\text{Li}_6$  structures ( $C_{2v,a}$  vs  $D_{4h}$  and  $C_s$  vs  $C_{5v}$ ). Binding energies are up to 2.5 kcal/mol smaller for the impure clusters (Tables 4 and 6), an observation already pointed out by Desphande.

The results listed in Tables 5 and 6, together with the negligible differences between the MP2/6-311g(d) and MP2/6-311+g(d) geometries for the bimetallic clusters, are in excellent agreement with the observation by Temelso and Sherrill<sup>13</sup> that for the particular clusters under consideration, inclusion of diffuse functions on the basis set has no practical consequences.

#### 4. Conclusions and Perspectives

We used an adapted version of the simulated annealing algorithm with a modified Metropolis test to produce initial guesses for structures in small  $\text{Li}_n^q$  ( $n = 5, 6, 7; q = 0, \pm 1$ ) and  $\text{Li}_5\text{Na}$  clusters in their lowest spin states. The algorithm calls an external program to calculate the quantum energy of randomly generated points in the conformational space. Structures are only rejected if a particular move results in raising the energy and in  $|\Delta E/E_j|$  being larger than Boltzmann's probability for  $\Delta E$ . Even at these small sizes, a total of 10 structures never before reported in the literature were found for the lithium clusters, and four new structures are reported for the  $\text{Li}_5\text{Na}$  clusters. Our CCSD(T)/6-311g(d)//MP2/6-311g(d) approach locates the correct global minimum on each PES except for those cases where the energy difference is too small. The agreement between the relative and binding energies and other properties reported here and those found elsewhere gives us confidence that the ASCEC program is predicting high-quality initial guesses for known cluster geometries, besides producing a few extra unknown configurations. The good results obtained also suggest that calculating the quantum energy during the simulations is an adequate approach, as it gives a better account of electron interaction than less accurate methods. Application of the algorithm bypasses the process of structure guessing when determining the stationary points within a given PES.

The overall satisfactory results encourage us to use the ASCEC program as a general tool to investigate other atomic and molecular clusters; at present, data relative to Na, Cu, Ag, and Au clusters are being processed in different documents to be published elsewhere. We also used the ASCEC program to study cooperative hydrogen-bond networks in water and methanol clusters and in their mixtures.

**Acknowledgment.** We are thankful to the Instituto de Física, Universidad de Antioquia, for ample provisions of computer time in the Hercules cluster. We also want to thank Prof. Jorge Zuluaga, the cluster administrator, for his help in installing the ASCEC program, for his patience in showing us the workings of the cluster, and for ensuring that the program always ran smoothly and efficiently. We also thank our student Diana Yepes for pointing out a few glitches in the original manuscript. E. Florez would like to thank Colciencias and the University of Antioquia for her PhD scholarship.

#### References and Notes

- (1) Florez, E.; Tiznado, W.; Mondragón, P.; Fuentealba, P. *J. Phys. Chem. A* **2005**, *109*, 7815.

- (2) Florez, E.; Mondragón, F.; Fuentealba, P. *J. Phys. Chem. B* **2006**, *110*, 13793.
- (3) Gonzales, S.; Sousa, C.; Fernandez-Garcia, M.; Berlin, V.; Illas, F. *J. Phys. Chem. B* **2002**, *106*, 7839.
- (4) Jarrold, M. *Science* **1991**, *252*, 1085.
- (5) Brown, W.; Brown, R.; Freeman, K.; Raghavachari, K.; Schluter, M. *Science* **1987**, *235*, 860.
- (6) Hayashi, S.; Kanzawa, Y.; Kataoka, M.; Nagarede, T.; Yamamoto, K. Z. *Physica D* **1993**, *26*, 144.
- (7) Florez, E.; Mondragón, F.; Truong, T.; Fuentealba, P. *Surf. Sci.* **2007**, *601*, 656.
- (8) Roy, A.; Thakkar, A. *Chem. Phys. Lett.* **2004**, *393*, 347.
- (9) Roy, A.; Thakkar, J. *J. Chem. Phys.* **2005**, *312*, 119.
- (10) Maheshwary, S.; Patel, N.; Sathyamurthy, N.; Kulkarni, A.; Gadres, S. *J. Phys. Chem.* **2001**, *105*, 10525.
- (11) Mejia, S.; Espinal, J.; Restrepo, A.; Mondragón, F. *J. Phys. Chem. A* **2007**, *111*, 8250.
- (12) Pérez, J.; Hadad, C.; Restrepo, A. *Int. J. Quantum Chem.* **2008**, in press (DOI: 10.1002/qua.21615).
- (13) Temelso, B.; Sherrill, D. *J. Chem. Phys.* **2005**, *122*, 064315.
- (14) Miyake, T.; Aida, M. *Int. Electron J. Mol. Des.* **2003**, *2*, 24.
- (15) Zope, R.; Baruah, T.; Pederson, M. *J. Comput. Methods Sci. Eng.* **2007**, *2*, 1.
- (16) Restrepo, A.; Marí, F.; González, C.; Márquez, M. *Quím., Actualidad Futuro* **1995**, *5*, 101.
- (17) Fletcher, R. *Practical Methods of Optimization*; Wiley, New York; Vol. 1, 1980.
- (18) Iannuzzi, M.; Laio, A.; Parrinello, M. *Phys. Rev. Lett.* **2003**, *90*, 238302.
- (19) Jellinek, J.; Srinivas, S.; Fantucci, P. *Chem. Phys. Lett.* **1998**, *288*, 705.
- (20) Bazterra, V.; Ona, O.; Caputo, M.; Ferraro, M.; Fuentealba, P.; Facelli, J. *Phys. Rev. A* **2004**, *69*, 053202.
- (21) Alexandrova, A.; Boldyrev, A. *J. Chem. Theory Comput.* **2005**, *1*, 566.
- (22) Tiznado, W.; Ona, O.; Bazterra, V.; Caputo, M.; Facelli, J.; Ferraro, M.; Fuentealba, P. *J. Chem. Phys.* **2005**, *123*, 214302.
- (23) Ona, O.; Bazterra, V.; Caputo, M.; Facelli, J.; Fuentealba, P.; Ferraro, M. *Phys. Rev. A* **2006**, *73*, 053203.
- (24) Gardet, G.; Rogemond, F.; Chermette, H. *J. Chem. Phys.* **1996**, *105*, 9933.
- (25) Sung, M.; Kawai, R.; Weare, K. *Phys. Rev. Lett.* **1994**, *73*, 3552.
- (26) Rousseau, R.; Marx, D. *Chem. Eur. J.* **2000**, *6*, 2982.
- (27) Rousseau, R.; Marx, D. *Phys. Rev. A* **1997**, *56*, 617.
- (28) Jones, R.; Liechtenstein, A.; Hutter, J. *J. Chem. Phys.* **1997**, *106*, 4566.
- (29) Boustani, I.; Pewerstoff, W.; Fantucci, P.; Bonačić-Koutecký, V.; Koutecký, J. *Phys. Rev. B* **1987**, *35* (18), 9437.
- (30) Bonačić-Koutecký, V.; Fantucci, P.; Koutecký, J. *Phys. Rev. B* **1988**, *37*, 4369.
- (31) Bonačić-Koutecký, V.; Fantucci, P.; Koutecký, J. *Chem. Rev.* **1991**, *91*, 1035.
- (32) Koutecký, J.; Boustani, I.; Bonačić-Koutecký, V. *Int. J. Quantum Chem.* **1990**, *38*, 149.
- (33) Grassi, A.; Lombardo, G.; Angilella, G.; March, N.; Pucci, R. *J. Chem. Phys.* **2004**, *120*, 11615.
- (34) Wheeler, S.; Sattelmeyer, P.; Schleyer, R.; Schaefer, H., III *J. Chem. Phys.* **2004**, *120*, 4683.
- (35) McAdon, M.; Goddard, W. *Phys. Rev. Lett.* **1985**, *55*, 2563.
- (36) McAdon, M.; Goddard, W. *J. Non-Cryst. Solids* **1985**, *75*, 149.
- (37) McAdon, M.; Goddard, W. *J. Phys. Chem.* **1987**, *91*, 2607.
- (38) Fantucci, P.; Bonačić-Koutecký, V.; Jellinek, J.; Wiechert, M.; Harrison, R.; Guest, M. *Chem. Phys. Lett.* **1996**, *250*, 47.
- (39) Rousseau, R.; Marx, D. *Phys. Rev. Lett.* **1998**, *80*, 2574.
- (40) Rousseau, R.; Marx, D. *J. Chem. Phys.* **1999**, *111*, 5091.
- (41) Ishikawa, Y.; Sugita, Y.; Nishikawa, T.; Okamoto, Y. *Chem. Phys. Lett.* **2001**, *333*, 199.
- (42) Fantucci, P.; Polezzo, S.; Bonačić-Koutecký, V.; Koutecký, J. *J. Chem. Phys.* **1990**, *92*, 6645.
- (43) Koutecký, J.; Fantucci, P. *Chem. Rev.* **1986**, *86*, 538.
- (44) Bonačić-Koutecký, V.; Boustani, I.; Guest, M.; Koutecký, J. *J. Chem. Phys.* **1988**, *89*, 4861.
- (45) Boustani, I.; Koutecký, J. *J. Chem. Phys.* **1988**, *89*, 5657.
- (46) Visser, S.; Alpert, Y.; Danovich, D.; Shaik, S. *J. Phys. Chem. A* **2000**, *104*, 11223.
- (47) Blanc, J.; Bonačić-Koutecký, V.; Broyer, M.; Chevaleyre, J.; Dugourd, P.; Koutecký, J.; Scheuch, C.; Wolf, J.; Wöste, L. *J. Chem. Phys.* **1992**, *96*, 1793.
- (48) Dugourd, P.; Blanc, J.; Bonačić-Koutecký, V.; Broyer, M.; Chevaleyre, J.; Koutecký, J.; Pittner, J.; Wolf, J.; Wöste, L. *Phys. Rev. Lett.* **1991**, *67* (19), 2638.
- (49) Metropolis, N.; Rosenbluth, A.; Rosenbluth, M.; Teller, A.; Teller, E. *J. Chem. Phys.* **1953**, *21*, 1087.
- (50) Kirkpatrick, S.; Gellat, C.; Vecchi, M. *Science* **1983**, *220*, 671.
- (51) Aarts, E.; Laarhoven, H. *Simulated Annealing: Theory and Applications*; Springer: New York, 1987.
- (52) Perez, M. F.; Restrepo, A. ASCEC V-01: Annealing Simulado Con Energía Cuántica. Property, Development and Implementation; Grupo de Química-Física Teórica, Instituto de Química, Universidad de Antioquia, AA 1226 Medellín, Colombia.
- (53) Frisch, M. J.; Trucks, G. W.; Schlegel, H. B.; Scuseria, G. E.; Robb, M. A.; Cheeseman, J. R.; Montgomery, J. A., Jr.; Vreven, T.; Kudin, K. N.; Burant, J. C.; Millam, J. M.; Iyengar, S. S.; Tomasi, J.; Barone, V.; Mennucci, B.; Cossi, M.; Scalmani, G.; Rega, N.; Petersson, G. A.; Nakatsuji, H.; Hada, M.; Ehara, M.; Toyota, K.; Fukuda, R.; Hasegawa, J.; Ishida, M.; Nakajima, T.; Honda, Y.; Kitao, O.; Nakai, H.; Klene, M.; Li, X.; Knox, J. E.; Hratchian, H. P.; Cross, J. B.; Bakken, V.; Adamo, C.; Jaramillo, J.; Gomperts, R.; Stratmann, R. E.; Yazyev, O.; Austin, A. J.; Cammi, R.; Pomelli, C.; Ochterski, J. W.; Ayala, P. Y.; Morokuma, K.; Voth, G. A.; Salvador, P.; Dannenberg, J. J.; Zakrzewski, V. G.; Dapprich, S.; Daniels, A. D.; Strain, M. C.; Farkas, O.; Malick, D. K.; Rabuck, A. D.; Raghavachari, K.; Foresman, J. B.; Ortiz, J. V.; Cui, Q.; Baboul, A. G.; Clifford, S.; Cioslowski, J.; Stefanov, B. B.; Liu, G.; Liashenko, A.; Piskorz, P.; Komaromi, I.; Martin, R. L.; Fox, D. J.; Keith, T.; Al-Laham, M. A.; Peng, C. Y.; Nanayakkara, A.; Challacombe, M.; Gill, P. M. W.; Johnson, B.; Chen, W.; Wong, M. W.; Gonzalez, C.; Pople, J. A. *Gaussian 03, Revision D.01*; Gaussian, Inc., Wallingford CT, 2004.
- (54) Dunning, T.; Hay, P. *Modern Theoretical Chemistry*; Plenum: New York, 1976; pp 1–28.
- (55) Hay, P.; Wadt, W. *J. Chem. Phys.* **1985**, *82*, 270.
- (56) Wadt, W.; Hay, P. *J. Chem. Phys.* **1985**, *82*, 284.
- (57) Hay, P.; Wadt, W. *J. Chem. Phys.* **1985**, *82*, 299.
- (58) Restrepo, A. Ph.D. Thesis; University of Connecticut, 2005.
- (59) The final structures still belong to the  $C_1$  point group, as that is the symmetry of choice during the optimization, so geometrical parameters may differ near the last decimal places.
- (60) Brechignac, C.; Busch, H.; Cahuzac, P.; Leygnier, J. *J. Chem. Phys.* **1994**, *101*, 6992.
- (61) Dugourd, P.; Rayane, D.; Labastie, P.; Vezin, B.; Chevaleyre, J.; Broyer, M. *Chem. Phys. Lett.* **1992**, *197*, 433.
- (62) Rayane, D.; Allouche, A.; Benichou, E.; Antoine, R.; Aubert, M.; Dugourd, P.; Broyer, M.; Rosti, C.; Chandezon, F.; Hubert, B.; Guet, C. *Eur. Phys. J. D* **1999**, *9*, 243.
- (63) Chandrakumar, K.; Ganthy, T.; Ghosh, S. *Int. J. Quantum Chem.* **2005**, *105*, 166.
- (64) Fuentealba, P. *Theoretical Calculations of the Static Dipole Polarizability of Atoms and Small Atomic Clusters, in Atoms, Molecules and Clusters in Electric Fields*; Maroulis, G. Ed.; Imperial College Press: London, 2006.
- (65) Desphande, M.; Kanhere, D.; Vasiliev, I.; Martin, R. *Phys. Rev. A* **2002**, *65*, 33202.